

Implications of texture zeros for a variant of tribimaximal mixing

Sanjeev Kumar*

*Department of Physics and Astrophysics, University of Delhi,
Delhi -110007, INDIA.*

Radha Raman Gautam†

Department of Physics, Himachal Pradesh University, Shimla -171005, INDIA.

(Dated: March 12, 2022)

We study the phenomenological implications of the presence of two texture zeros in the neutrino mass matrix assuming that the neutrino mixing matrix has its first column identical to that of the tribimaximal mixing matrix. Only two patterns of this kind are compatible with the experimental data. These textures have definite predictions for the neutrino observables that are testable in future neutrino experiments.

PACS numbers: 11.30.Hv, 12.15.Ff, 14.60.Pq

In the recent years, considerable efforts have been put towards determining the structure of the neutrino mass matrix (M_ν) [1]. The non-zero value of the reactor mixing angle θ_{13} , recently determined in various neutrino oscillation experiments [2], has called many neutrino mass models predicting $\theta_{13} = 0$ into question. The models based upon the Tribimaximal (TBM) [3] mixing, that predicted the reactor, atmospheric and solar mixing angles as $\theta_{13} = 0$, $\theta_{23} = \frac{\pi}{2}$, and $\theta_{12} = \arctan(1/\sqrt{2})$, respectively, need modifications in the light of a non-zero θ_{13} . The TBM mixing matrix is given as

$$U_{\text{TBM}} = \begin{pmatrix} \sqrt{\frac{2}{3}} & \frac{1}{\sqrt{3}} & 0 \\ -\frac{1}{\sqrt{6}} & \frac{1}{\sqrt{3}} & \frac{1}{\sqrt{2}} \\ -\frac{1}{\sqrt{6}} & \frac{1}{\sqrt{3}} & -\frac{1}{\sqrt{2}} \end{pmatrix}. \quad (1)$$

Many ways have been proposed to modify the TBM ansatz to accommodate a non-zero θ_{13} . A simple possibility is to keep one column of TBM mixing matrix unchanged while modifying its other two columns within unitarity constraints [4]. This gives rise to three Trimaximal (TM) mixing patterns, viz., TM_1 , TM_2 , and TM_3 , that have their first, second and third columns identical to TBM matrix, respectively [4]. These three mixing schemes contain TBM mixing as a special case that enlarges the symmetry of these mixing patterns. Hence, they could have been named TBM_1 , TBM_2 , and TBM_3 .

TM_1 mixing is given as

$$U_{\text{TM}_1} = \begin{pmatrix} \frac{2}{\sqrt{3}} & \frac{1}{\sqrt{3}} \cos \theta & \frac{1}{\sqrt{3}} \sin \theta \\ -\frac{1}{\sqrt{6}} & \frac{1}{\sqrt{3}} \cos \theta - \frac{e^{i\phi} \sin \theta}{\sqrt{2}} & \frac{1}{\sqrt{3}} \sin \theta + \frac{e^{i\phi} \cos \theta}{\sqrt{2}} \\ -\frac{1}{\sqrt{6}} & \frac{1}{\sqrt{3}} \cos \theta + \frac{e^{i\phi} \sin \theta}{\sqrt{2}} & \frac{1}{\sqrt{3}} \sin \theta - \frac{e^{i\phi} \cos \theta}{\sqrt{2}} \end{pmatrix}. \quad (2)$$

The mixing scheme reduces to the TBM scheme in the special case $\theta = 0$ and $\phi = 0$.

TM_2 mixing is given as

$$U_{\text{TM}_2} = \begin{pmatrix} \sqrt{\frac{2}{3}} \cos \theta & \frac{1}{\sqrt{3}} & \sqrt{\frac{2}{3}} \sin \theta \\ -\frac{\cos \theta}{\sqrt{6}} + \frac{e^{-i\phi} \sin \theta}{\sqrt{2}} & \frac{1}{\sqrt{3}} & -\frac{\sin \theta}{\sqrt{6}} - \frac{e^{-i\phi} \cos \theta}{\sqrt{2}} \\ -\frac{\cos \theta}{\sqrt{6}} - \frac{e^{-i\phi} \sin \theta}{\sqrt{2}} & \frac{1}{\sqrt{3}} & -\frac{\sin \theta}{\sqrt{6}} + \frac{e^{-i\phi} \cos \theta}{\sqrt{2}} \end{pmatrix}. \quad (3)$$

The mixing scheme reduces to the TBM scheme in the special case $\theta = 0$ and $\phi = 0$. This mixing scheme corresponds to the magic symmetry.

TM_3 mixing is given as

$$U_{\text{TM}_3} = \begin{pmatrix} \cos \theta & \sin \theta & 0 \\ -\frac{e^{-i\phi} \sin \theta}{\sqrt{2}} & \frac{e^{-i\phi} \cos \theta}{\sqrt{2}} & \frac{1}{\sqrt{2}} \\ -\frac{e^{-i\phi} \sin \theta}{\sqrt{2}} & \frac{e^{-i\phi} \cos \theta}{\sqrt{2}} & -\frac{1}{\sqrt{2}} \end{pmatrix}. \quad (4)$$

The mixing scheme reduces to the TBM scheme in the special case $\theta = \arctan(1/\sqrt{2})$ and $\phi = 0$. This mixing scheme is equivalent to $\mu - \tau$ symmetry.

Another simple assumption that can accommodate a non-zero θ_{13} is the presence of texture zeros in the neutrino mass matrix [5–7]. Texture zeros induce relations between mixing matrix elements and neutrino masses. Considering neutrinos to be Majorana fermions and working in a basis where the charged lepton mass matrix M_l is diagonal, there are in total fifteen different patterns of two texture zeros in the neutrino mass matrices. Out of these fifteen possible patterns, only seven can satisfy the present neutrino oscillation data [5, 6]. These seven patterns are classified in three classes A, B and C corresponding to the normal, quasi-degenerate and inverted mass hierarchies of neutrinos [Table I].

The current neutrino data are consistent with the possibility of keeping first or second column of the mixing matrix unmodified (TM_1 or TM_2 mixing) while modifying other columns within unitarity constraints. The experimental data is also consistent with the presence of two texture zeros in the neutrino mass matrix. If we combine both approaches together by having texture zeros in a mass matrix corresponding to TM_1 or TM_2 mixing, we

* skverma@physics.du.ac.in

† gautamrrg@gmail.com

Type	Constraining Equations
A ₁	$M_{ee} = 0, M_{e\mu} = 0$
A ₂	$M_{ee} = 0, M_{e\tau} = 0$
B ₁	$M_{e\tau} = 0, M_{\mu\mu} = 0$
B ₂	$M_{e\mu} = 0, M_{\tau\tau} = 0$
B ₃	$M_{e\mu} = 0, M_{\mu\mu} = 0$
B ₄	$M_{e\tau} = 0, M_{\tau\tau} = 0$
C	$M_{\mu\mu} = 0, M_{\tau\tau} = 0$

TABLE I. Seven allowed mass matrices with two zeros classified into three classes.

are bound to get very predictive neutrino mass matrices. In an earlier work [9], we studied the implications of two texture zeros in a magic mass matrix giving TM₂ mixing. In the present work, we study the phenomenological implications of the presence of two texture zeros in a neutrino mass matrix giving TM₁ mixing.

A mass matrix giving TM₁ mixing can be parameterized as

$$M_{\text{TM}_1} = \begin{pmatrix} 2a & 2b & 2c \\ 2b & b-c+d & 2a+2b-d \\ 2c & 2a+2b-d & -3b+3c+d \end{pmatrix}. \quad (5)$$

We can obtain the form of the neutrino mass matrix giving TM₁ mixing for the seven patterns of two texture zeros by substituting the respective constraints from Table I in Eq. (5).

The neutrino mass matrix of type A₁ giving TM₁ mixing is given as

$$M^{A_1} = \begin{pmatrix} 0 & 0 & 2c \\ 0 & -2c+\Delta & c-\Delta \\ 2c & c-\Delta & 2c+\Delta \end{pmatrix} \quad (6)$$

where $\Delta = d + b$. Similarly, the neutrino mass matrix of type A₂ giving TM₁ mixing is

$$M^{A_2} = \begin{pmatrix} 0 & 2b & 0 \\ 2b & 2b+\Delta & b-\Delta \\ 0 & b-\Delta & -2b+\Delta \end{pmatrix}, \quad (7)$$

where $\Delta = d - c$.

The four mass matrices giving TM₁ mixing for class B are

$$M^{B_1} = \begin{pmatrix} 2a & 2b & 0 \\ 2b & 0 & 2a+3b \\ 0 & 2a+3b & -4b \end{pmatrix}, \quad (8)$$

$$M^{B_2} = \begin{pmatrix} 2a & 0 & 2c \\ 0 & -4c & 2a+3c \\ 2c & 2a+3c & 0 \end{pmatrix}, \quad (9)$$

$$M^{B_3} = \begin{pmatrix} 2a & 0 & 2c \\ 0 & 0 & 2a-c \\ 2c & 2a-c & 4c \end{pmatrix}, \quad (10)$$

and

$$M^{B_4} = \begin{pmatrix} 2a & 2b & 0 \\ 2b & 4b & 2a-b \\ 0 & 2a-b & 0 \end{pmatrix}. \quad (11)$$

We will show that all these mass matrices of type class B giving TM₁ mixing are not allowed by the experimental data.

The mass matrix with TM₁ mixing for the class C is

$$M^C = \begin{pmatrix} 2a & 2b & 2b \\ 2b & 0 & 2a+2b \\ 2b & 2a+2b & 0 \end{pmatrix}. \quad (12)$$

This mass matrix has μ - τ symmetry and implies $\theta_{13} = 0$. Hence, it is not allowed.

The phenomenology of patterns A₁ and A₂ is related: one can obtain the predictions for A₂ by making the transformations [6, 7]

$$\theta_{23} \rightarrow \frac{\pi}{2} - \theta_{23}, \delta \rightarrow \pi - \delta \quad (13)$$

on the predictions of A₁. Hence, we study the phenomenological implications for pattern A₁ only.

Any mass matrix M giving TM₁ mixing can be diagonalized by a mixing matrix $U = U_{\text{TM}_1}$ given in Eq. (2) using the relation

$$U^T M U = M_{\text{diag}} \quad (14)$$

where M_{diag} is the diagonal mass matrix given as

$$M_{\text{diag}} = \begin{pmatrix} m_1 & 0 & 0 \\ 0 & e^{2i\alpha} m_2 & 0 \\ 0 & 0 & e^{2i\beta} m_3 \end{pmatrix}. \quad (15)$$

Here, m_1, m_2 , and m_3 are the neutrino masses and α and β are the two Majorana phases.

Once the mixing matrix U is known, the mixing angles can be calculated using the relations:

$$s_{12}^2 = \frac{|U_{12}|^2}{1 - |U_{13}|^2}, s_{23}^2 = \frac{|U_{23}|^2}{1 - |U_{13}|^2} \text{ and } s_{13}^2 = |U_{13}|^2, \quad (16)$$

where $s_{ij} = \sin \theta_{ij}$ and $c_{ij} = \cos \theta_{ij}$. For our case $U = U_{\text{TM}_1}$, the above relations give

$$s_{12}^2 = 1 - \frac{2}{3 - \sin^2 \theta}, \quad (17)$$

$$s_{23}^2 = \frac{1}{2} \left(1 + \frac{\sqrt{6} \sin 2\theta \cos \phi}{3 - \sin^2 \theta} \right), \quad (18)$$

and

$$s_{13}^2 = \frac{1}{3} \sin^2 \theta. \quad (19)$$

We see from Eq. (17) that θ_{12} is smaller than its TBM value $s_{12}^2 = 1/3$. In contrast, the value of θ_{12} is larger

than the TBM value for TM_2 mixing. Since the experimental value of θ_{12} is towards the lower side of the TBM value, TM_1 mixing is more appealing than TM_2 mixing.

The CP violating phase δ can be calculated from the Jarlskog rephasing invariant measure of CP violation [8]

$$J = \text{Im}(U_{11}U_{12}^*U_{21}^*U_{22}) \quad (20)$$

using the relation

$$J = s_{12}s_{23}s_{13}c_{12}c_{23}c_{13}^2 \sin \delta. \quad (21)$$

Substituting the elements of the TM_1 mixing matrix in Eq. (20), we obtain

$$J = \frac{1}{6\sqrt{6}} \sin 2\theta \sin \phi. \quad (22)$$

From Eqs. (21) and (22), we get

$$\cot^2 \delta = \cot^2 \phi - \frac{6 \sin^2 2\theta \cot^2 \phi}{(3 - \sin^2 \theta)^2}. \quad (23)$$

We reconstruct the neutrino mass matrix for TM_1 mixing using the relation:

$$M_\nu = U^* M_{\text{diag}} U^\dagger \quad (24)$$

where $U = U_{TM_1}$. To obtain the predictions for the neutrino mass matrix of the type A_1 given by Eq. (6), we have to solve the two complex equations: $M_{\nu_{11}} = 0$ and $M_{\nu_{12}} = 0$. Solving the equation $M_{\nu_{11}} = 0$, we get

$$\frac{m_1}{m_2} = \frac{\sin 2(\alpha - \beta) \cos^2 \theta}{2 \sin 2\beta} \quad (25)$$

and

$$\frac{m_2}{m_3} = -\frac{\sin 2\beta \tan^2 \theta}{\sin 2\alpha}. \quad (26)$$

Using these two equations, we evaluate m_1/m_3 and invert the resulting relation to obtain

$$\cot 2\alpha = \cot 2\beta + \frac{m_1}{m_3} \csc 2\beta \cot^2 \theta. \quad (27)$$

We note that the presence of a zero at (1,1) entry in a mass matrix with TM_1 mixing, through Eqs. (25) and (26), implies a beautiful sum-rule on neutrino masses:

$$\frac{\sin 2(\alpha - \beta)}{2m_1} - \frac{\sin 2\beta}{m_2} + \frac{\sin 2\alpha}{m_3} = 0. \quad (28)$$

The texture zero at (1,1) entry in a mass matrix with TM_1 mixing also gives a prediction for the ratio $r = \Delta m_{21}^2 / \Delta m_{31}^2$. From Eqs. (25) and (26), we obtain

$$r = \frac{-\sin^2 2(\alpha - \beta) + 4 \sec^4 \theta \sin^2 2\beta}{-\sin^2 2(\alpha - \beta) + 4 \csc^4 \theta \sin^2 2\beta}. \quad (29)$$

We solve the second equation $M_{\nu_{12}} = 0$ by equating its real and imaginary parts to zero. We eliminate m_1

and m_2 from the resulting equations using Eqs. (25) and (26). Equating the imaginary part of $M_{\nu_{12}}$ to zero, we obtain

$$\sin^2 \theta = -\frac{\sin 2\alpha \sin(2\beta - \phi)}{\sin 2(\alpha - \beta) \sin \phi}. \quad (30)$$

We get a quadratic equation in $\tan^2 \theta$ on equating the real part of $M_{\nu_{12}}$ to zero:

$$\frac{\sqrt{6} \sin 2\beta \cos(2\alpha - \phi)}{\sin 2(\alpha - \beta)} \tan^2 \theta + 3 \tan \theta + \frac{\sqrt{6} \sin 2\alpha \cos(2\beta - \phi)}{\sin 2(\alpha - \beta)} = 0. \quad (31)$$

Solving this equation by substituting α from Eq. (27), we obtain

$$\tan \theta = \sqrt{\frac{3 \sin(2\beta - \phi)}{2 \sin 2\beta}}. \quad (32)$$

The value of θ calculated in Eqs. (30) and (32) must be identical. This requirement gives

$$\cot 2\alpha = \cot \phi + \frac{2 \sin 2\beta}{3 \sin(2\beta - \phi) \sin \phi}. \quad (33)$$

Equations (25), (26), (32) and (33) are the four predictions for the neutrino mass matrix of type A_1 . We can express these four predictions as expressions for α , β , $\frac{m_1}{m_2}$, $\frac{m_2}{m_3}$ as functions of θ and ϕ . Inversion of Eq. (32) gives

$$\cot 2\beta = \cot \phi - \sqrt{\frac{2}{3}} \csc \phi \tan \theta. \quad (34)$$

Substituting β from Eq. (34) in Eq. (33) gives

$$\cot 2\alpha = \cot \phi + \sqrt{\frac{2}{3}} \csc \phi \cot \theta. \quad (35)$$

Equations(25) and (26) after substituting values of α and β give

$$\frac{m_2^2}{m_1^2} = 5 \sec^2 \theta + 4\sqrt{6} \tan \theta \cos \phi + \tan^2 \theta - 1 \quad (36)$$

and

$$\frac{m_3^2}{m_1^2} = 6 \csc^2 \theta - 4\sqrt{6} \cot \theta \cos \phi - 2. \quad (37)$$

We can use these ratios to calculate $r = \frac{\Delta m_{21}^2}{\Delta m_{31}^2}$ as a function of θ and ϕ or we can calculate it directly from Eq. (29). We obtain

$$r = \frac{3 - 6 \sec^2 \theta - 4\sqrt{6} \tan \theta \cos \phi}{3 - \csc \theta + 4\sqrt{6} \cot \theta \cos \phi}. \quad (38)$$

For TM_2 mixing, we have $r = \tan^2 \theta$ [9]. In contrast, r is function of both θ and ϕ for TM_1 mixing. By demanding

that r satisfies its experimental value, one can calculate experimentally allowed values of ϕ .

Once the experimentally allowed values of θ and ϕ are known, the observables $\theta_{12}, \theta_{23}, \theta_{13}$ and δ can be calculated from Eqs. (17), (18), (19) and (23) as they are functions of θ and ϕ .

The experimentally allowed value of θ can be calculated from Eq. (19) using the experimental value of $\sin^2 \theta_{13} = 0.0216 \pm 0.00075$ [10]. We get $\theta = 14.78 \pm 0.26$ degrees. We could have also used the experimental value of $\sin^2 \theta_{12} = 0.306 \pm 0.012$ [10] to constrain θ . However, this gives a larger range of θ . We plot r as a function of ϕ using Eq. (38) for $\theta = 14.78 \pm 0.26$ degrees in Fig. 1. From the experimental values $\Delta m_{21}^2 = (7.50 \pm 0.19) \times 10^{-5}$ eV² and $\Delta m_{31}^2 = (2.524 \pm 0.04) \times 10^{-3}$ eV² [10], we get the experimental value $r = 0.0297 \pm 0.0003$. Here, all the experimental errors are at one standard deviation. We find that the predicted and experimental values of r are consistent only for two regions of ϕ depicted in Fig. 1. In this way, we can constrain both θ and ϕ . Then, all other observables can be obtained as they are functions of θ and ϕ .

A better approach is to constrain θ and ϕ by minimizing the χ^2 -function

$$\chi^2(\theta, \phi) = \sum_{i=1}^3 \left[\frac{v_i(\theta, \phi) - v_i^{exp}}{\sigma_i^{exp}} \right]^2 \quad (39)$$

where the variables $v_i = (\sin^2 \theta_{12}, \sin^2 \theta_{13}, r)$; v_i^{exp} are experimental values of v_i ; and σ_i^{exp} are the standard deviations in the experimental values of v_i . The $\chi^2(\theta, \phi)$ is minimum at $\theta = 14.8$ degrees and $\phi = 103.2$ degrees or $\phi = 256.8$ degrees. The minimum value is $\chi_{min}^2 = 1.8$. The contours of $\Delta\chi^2 = \chi^2 - \chi_{min}^2$ corresponding to 1σ , 2σ , and 3σ confidence level are shown in Fig. 2. The predictions for θ_{23} and δ for TM₁ mixing in pattern A₁ have been shown in Fig. 3 at various confidence levels. The predictions for TM₁ mixing in pattern A₂ can be obtained by using the transformations given in Eq. (13). We find that δ is predicted either around 100° or around 260° with a spread of around 10° . Table II shows the 3σ ranges of δ and θ_{23} for these two solutions obtained from our analysis. The mixing angle θ_{23} lies below (above) 45° for pattern A₁ (A₂).

Recently, long baseline neutrino oscillation experiments like MINOS and T2K [11] are showing a preference for the CP violating phase δ to be around 270° . In particular, a recent global analysis in Ref. [10] rules out δ from about 55° to 120° at 3σ CL for inverted mass ordering. A certain portion of δ is also ruled out if $\theta_{23} < 45^\circ$ for the normal mass ordering (see Fig. 11 in Ref. [10]). In our χ^2 analysis, we do not put any experimental constraints on δ and θ_{23} as these parameters are not precisely measured and their distributions are not Gaussian. If we take into consideration the limits on δ as given in Ref. [10], the Solution - I in Table II for pattern A₁ is ruled out and only Solution - II, where δ lies around 260° , remains compatible. Since the exclusion region of

Type	θ_{23}	δ	
		Solution - I	Solution - II
A ₁	41.18° - 44.02°	94.6° - 106.5°	253.5° - 265.5°
A ₂	45.98° - 48.82°	73.5° - 85.5°	274.6° - 286.5°

TABLE II. Allowed 3σ ranges of θ_{23} and δ for patterns A₁ and A₂. Solution - I and Solution - II are two allowed solutions for δ .

δ with respect to θ_{23} for normal mass spectrum (Fig. 11 of Ref. [10]) is not symmetric around $\theta_{23} = 45^\circ$, both solutions are still allowed for pattern A₂.

The predictions for Majorana phases α and β are shown in Fig. 4. We also depict the predictions for the effective electron neutrino mass for β -decay $m_\beta^2 = m_1^2 |U_{e1}|^2 + m_2^2 |U_{e2}|^2 + m_3^2 |U_{e3}|^2$ and the sum of neutrino masses $\sum m_i = m_1 + m_2 + m_3$ in Fig. 5. Since the (1,1) element of the neutrino mass matrix vanishes for patterns A₁ and A₂, this leads to a vanishing effective Majorana neutrino mass ($|M_{ee}| = |m_1 U_{e1}^2 + m_2 U_{e2}^2 + m_3 U_{e3}^2|$) for these patterns.

The neutrino mass matrix of type B₁ has zeros at (1, 3) and (2, 2) entries. This implies following expression of ratio r in the presence of TM₁ mixing:

$$r = \frac{1}{6} \left(2\sqrt{6} \sin(2\theta) \cos(\phi) + 9 \cos(2\theta) - 3 \right). \quad (40)$$

We can express θ in terms of θ_{13} using Eq. (19) in the above relation expressing r as a function of θ (Fig. 6). It is clear that we cannot have both r and θ_{13} in their experimentally allowed ranges simultaneously. Hence, this pattern is inconsistent with the experimental data when combined with TM₁ mixing. The neutrino mass matrix of type B₂ is related to the neutrino mass matrix of type B₁ by a μ - τ exchange [6, 7] and has identical predictions for r and θ_{13} . Hence, neutrino mass matrix of type B₂ with TM₁ mixing is also incompatible with the recent experimental data.

The neutrino mass matrix of type B₃ has zeros at (1, 2) and (2, 2) entries. The expression of ratio r in the presence of TM₁ mixing is given by

$$r = \frac{1}{10} \left(-2\sqrt{6} \sin(2\theta) \cos(\phi) - \cos(2\theta) - 5 \right). \quad (41)$$

In case of pattern B₃, the parameter r always remains larger than 0.4 whereas the experimental range of this parameter lies well below the value 0.4 (see Fig. 6). Thus pattern B₃ is also incompatible with the experimental data. Since pattern B₃ is related to pattern B₄ by μ - τ exchange symmetry, the pattern B₄ is also incompatible with the experimental data when combined with TM₁ mixing.

In conclusion, we have studied the phenomenological implications of two texture zeros in the presence of TM₁ mixing. There are seven allowed patterns for the presence of two texture zeros in the neutrino mass matrix. The

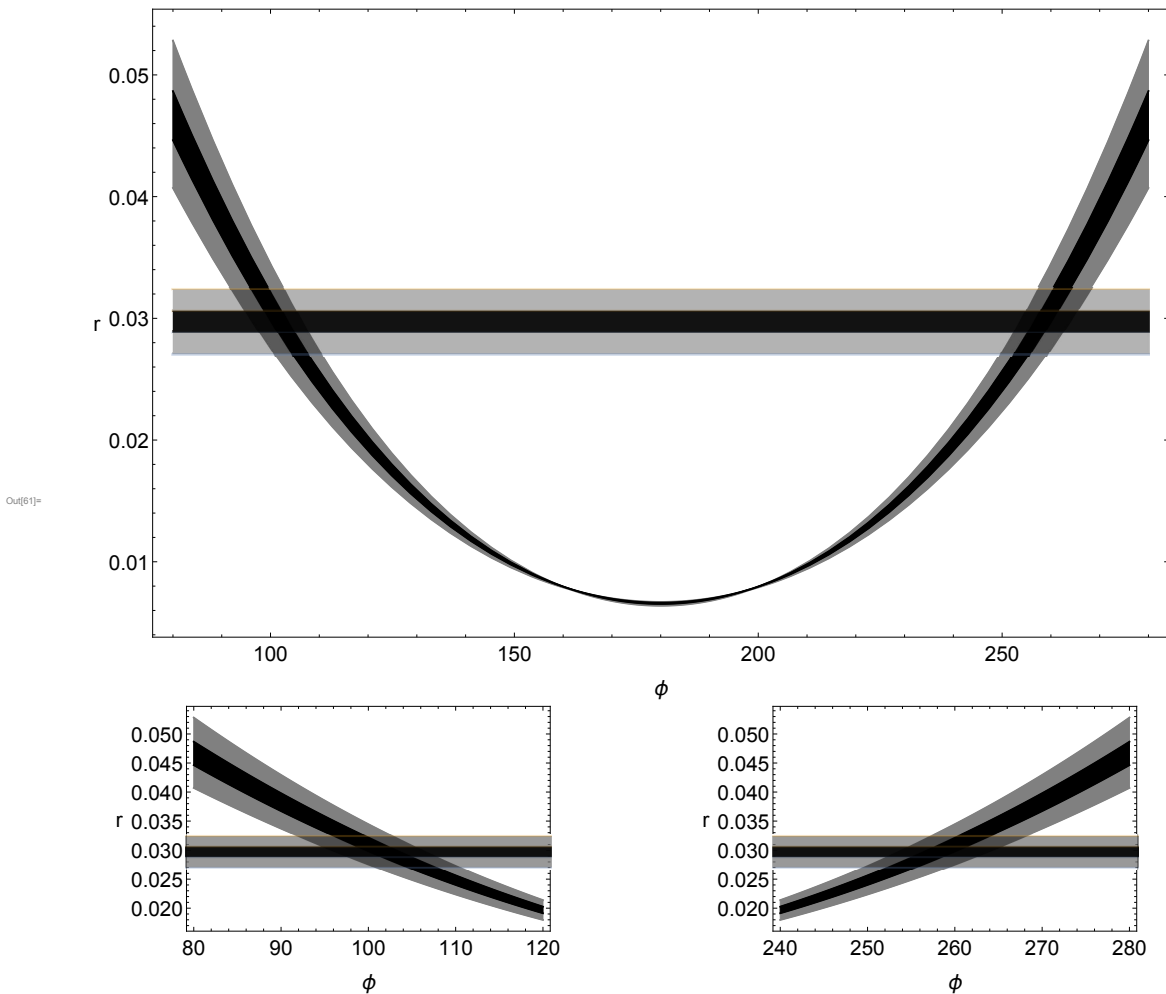


FIG. 1. The ratio $r = \Delta m_{12}^2/\Delta m_{13}^2$ as a function of ϕ (degrees). The horizontal line depicts the experimental value of r . The inner solid bands depict the 1σ range and the outer gray bands depict the 3σ range.

presence of TM_1 mixing rules out five out of the seven patterns of two texture zeros. The neutrino mass matrix having two texture zeros and TM_1 mixing simultaneously can only belong to patterns A_1 and A_2 . The Dirac CP violating phase δ is restricted to two narrow regions around 100° and 260° for these patterns. For TM_1 mixing, θ_{12} is smaller than its TBM value and moves towards its best fit value with the increase in θ . The imposition of TM_1 mixing on two zeros make these classes very predictive and these predictions can be tested in future neutrino

oscillation experiments.

ACKNOWLEDGMENTS

R. R. G. acknowledges the financial support provided by Department of Science and Technology, Government of India under the Grant No. SB/FTP/PS-128/2013.

-
- [1] A. Strumia and F. Vissani, [hep-ph/0606054]; R. N. Mohapatra *et al.*, Rept. Prog. Phys. **70**, 1757 (2007), [hep-ph/0510213]; M. C. Gonzalez-Garcia and M. Maltoni, Phys. Rept. **460**, 1 (2008), [arXiv:0704.1800 [hep-ph]]; S. F. King, A. Merle, S. Morisi, Y. Shimizu and M. Tanimoto, New J. Phys. **16**, 045018 (2014), [arXiv:1402.4271 [hep-ph]].
- [2] K. Abe et al. [T2K Collaboration], Phys. Rev. Lett. **107**,

041801 (2011), [arXiv:1106.2822 [hep-ex]]; P. Adamson et al. [MINOS Collaboration], Phys. Rev. Lett. **107**, 181802 (2011), [arXiv:1108.0015 [hep-ex]]; Y. Abe et al. [Double Chooz Collaboration], Phys. Rev. Lett. **108**, 131801 (2012), [arXiv:1112.6353 [hep-ex]]; F. P. An et al., [Daya Bay Collaboration], Phys. Rev. Lett. **108**, 171803 (2012), [arXiv:1203.1669 [hep-ex]]; Soo-Bong Kim, for RENO Collaboration, Phys. Rev. Lett. **108**, 191802 (2012),

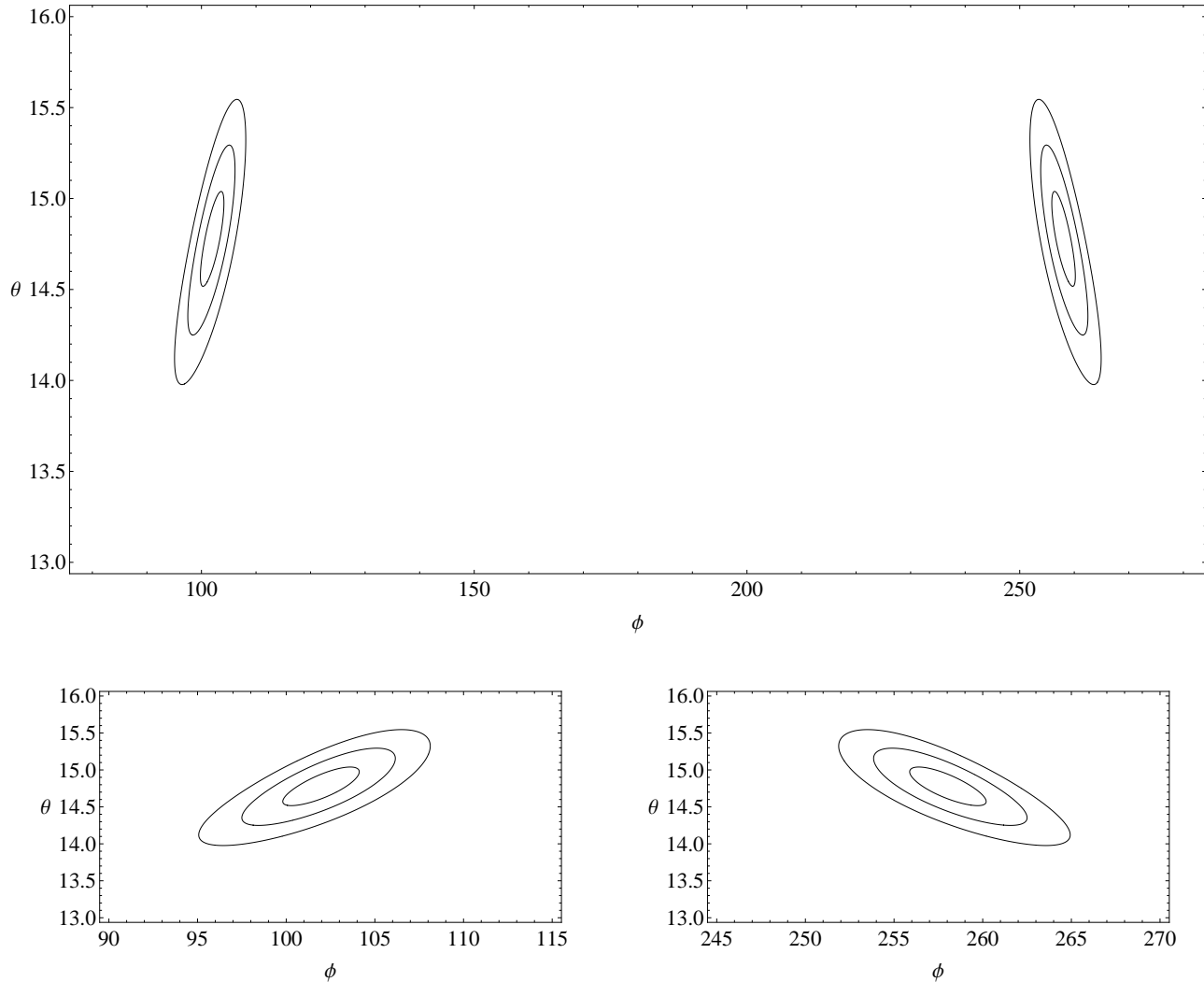


FIG. 2. The allowed region on $(\theta - \phi)$ parameter space. The contours are at 1, 2, and 3 σ confidence levels (CL) and all the angles are in degrees.

- [arXiv:1204.0626 [hep-ex]].
- [3] P. F. Harrison, D. H. Perkins and W. G. Scott, *Phys. Lett. B* **530**, 167 (2002), [hep-ph/0202074]; Zhi-zhong Xing, *Phys. Lett. B* **533**, 85 (2002), [hep-ph/0204049]; P. F. Harrison and W. G. Scott, *Phys. Lett. B* **535**, 163 (2002), [hep-ph/0203209].
- [4] J. D. Bjorken, P. F. Harrison and W. G. Scott, *Phys. Rev. D* **74**, 073012 (2006), [hep-ph/0511201]; X. G. He and A. Zee, *Phys. Lett. B* **645**, 427 (2007), [hep-ph/0607163]; Carl H. Albright, Werner Rodejohann *Eur.Phys.J. C* **62** (2009) 599-608 [arXiv:0812.0436 [hep-ph]]; Carl H. Albright, Alexander Dueck, Werner Rodejohann *Eur.Phys.J. C* **70** (2010) 1099-1110, [arXiv:1004.2798 [hep-ph]]; X. G. He and A. Zee, *Phys. Rev. D* **84**, 053004 (2011), [arXiv:1106.4359 [hep-ph]]; Sanjeev Kumar, *Phys.Rev.D* **82** (2010) 013010, [arXiv:1007.0808 [hep-ph]]; *ibid* **88** (2013) 1, 016009, [arXiv:1305.0692 [hep-ph]]; S. Gupta, A. S. Joshipura and K. M. Patel, *Phys. Rev. D* **85**, 031903 (2012), [arXiv:1112.6113 [hep-ph]].
- [5] Paul H. Frampton, Sheldon L. Glashow and Danny Marfatia, *Phys. Lett. B* **536**, 79 (2002), [hep-ph/0201008].
- [6] H. Fritzsch, Zhi-zhong Xing, S. Zhou, *JHEP* **1109**, 083 (2011), [arXiv:1108.4534 [hep-ph]].
- [7] Zhi-zhong Xing, *Phys. Lett. B* **530**, 159 (2002), [hep-ph/0201151]; Bipin R. Desai, D. P. Roy and Alexander R. Vaucher, *Mod. Phys. Lett. A* **18**, 1355 (2003), [hep-ph/0209035]; A. Merle, W. Rodejohann, *Phys. Rev D* **73**, 073012 (2006), [hep-ph/0603111]; S. Dev, Sanjeev Kumar, S. Verma and S. Gupta, *Nucl. Phys. B* **784**, 103 (2007), [hep-ph/0611313]; S. Dev, S. Kumar, S. Verma and S. Gupta, *Phys. Rev. D* **76**, 013002 (2007), [hep-ph/0612102]; G. Ahuja, S. Kumar, M. Randhawa, M. Gupta, S. Dev, *Phys. Rev. D* **76**, 013006 (2007), [hep-ph/0703005]; S. Kumar, *Phys. Rev. D* **84**, 077301 (2011), [arXiv:1108.2137 [hep-ph]]; S. Dev, S. Kumar, S. Verma, *Phys. Rev. D* **79**, 033011 (2009), [hep-ph/0901.2819]; P. O. Ludl, S. Morisi, E. Peinado, *Nucl.*

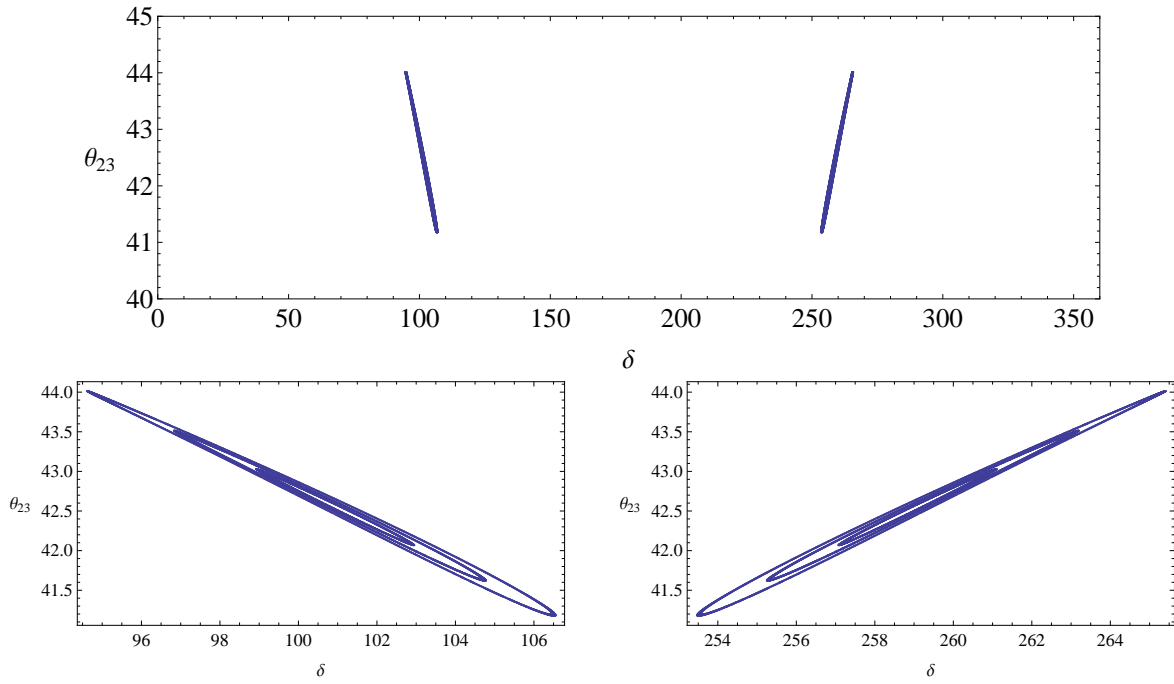


FIG. 3. The predictions for θ_{23} and δ at 1, 2, and 3 σ confidence levels where all the angles are in degrees.

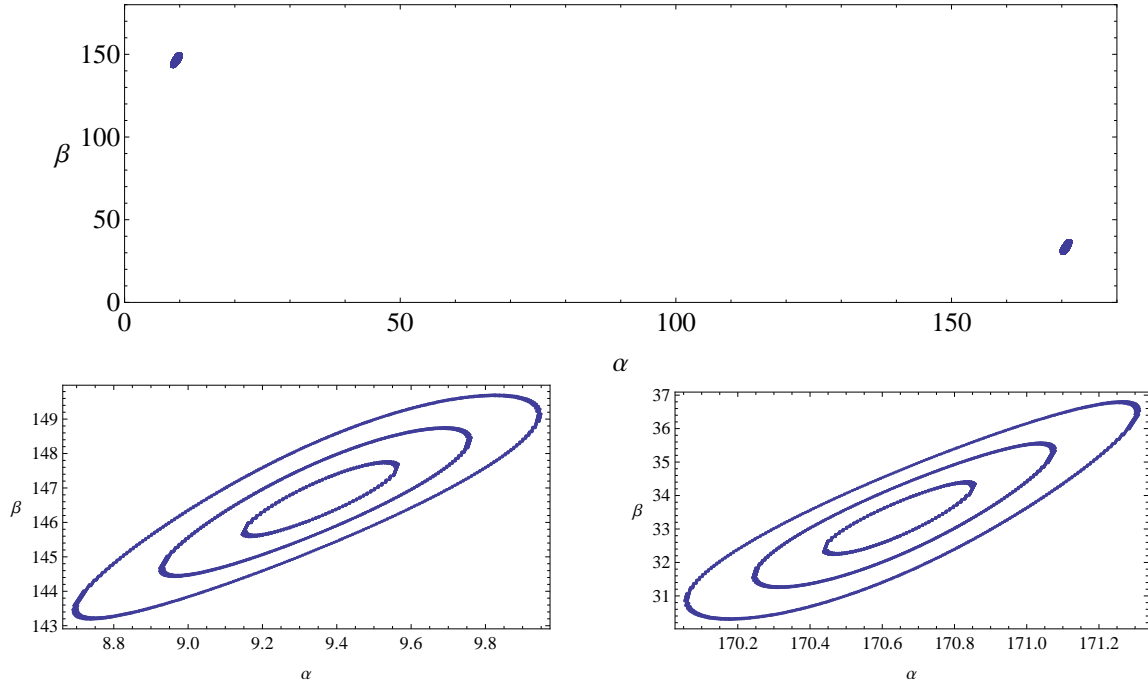


FIG. 4. Predictions for Majorana phases α and β at 1, 2, and 3 σ confidence levels where all the angles are in degrees.

Phys. B **857**, 411 (2012), [arXiv:1109.3393 [hep-ph]]; D. Meloni, G. Blankenburg, *Nucl. Phys. B* **867**, 749 (2013), [arXiv:1204.2706 [hep-ph]]; W. Grimus, P. O. Ludl, *J. Phys. G* **40**, 055003 (2013) [arXiv:1208.4515 [hep-ph]]; J. Liao, D. Marfatia, K. Whisnant, [arXiv:1311.2639 [hep-ph]]; D. Meloni, A. Meroni, E. Peinado, *Phys. Rev. D* **89** (2014) 053009, [arXiv:1401.3207 [hep-ph]]; S. Dev,

R. R. Gautam, L. Singh and M. Gupta, *Phys. Rev. D* **90**, no. 1, 013021 (2014), [arXiv:1405.0566 [hep-ph]]; G. Ahuja, S. Sharma, P. Fakay and M. Gupta, *Mod. Phys. Lett. A* **30**, 1530025 (2015), [arXiv:1604.03339 [hep-ph]]; M. Singh, G. Ahuja and M. Gupta, *PTEP* **2016**, no. 12, 123B08 (2016), [arXiv:1603.08083 [hep-ph]]; D. Borah, M. Ghosh, S. Gupta and S. K. Raut,

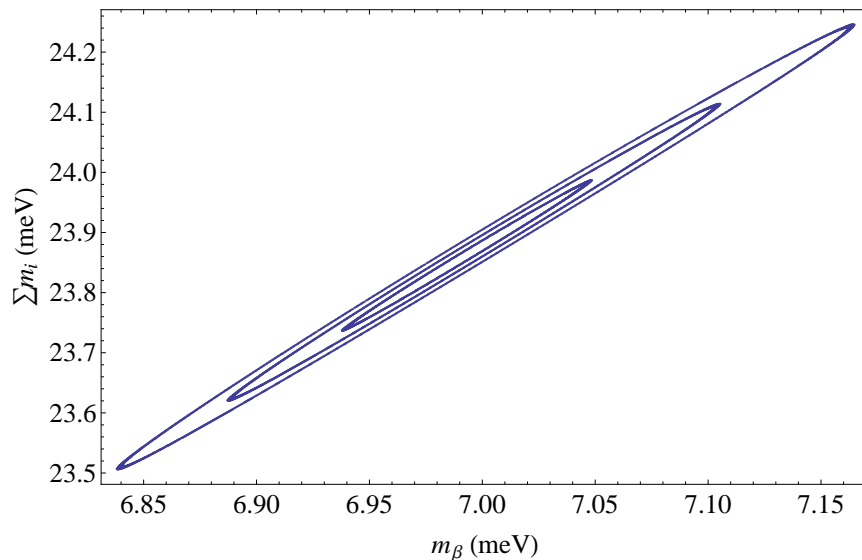


FIG. 5. Predictions for effective electron neutrino mass for β -decay and sum of neutrino masses at 1, 2, and 3 σ confidence levels.

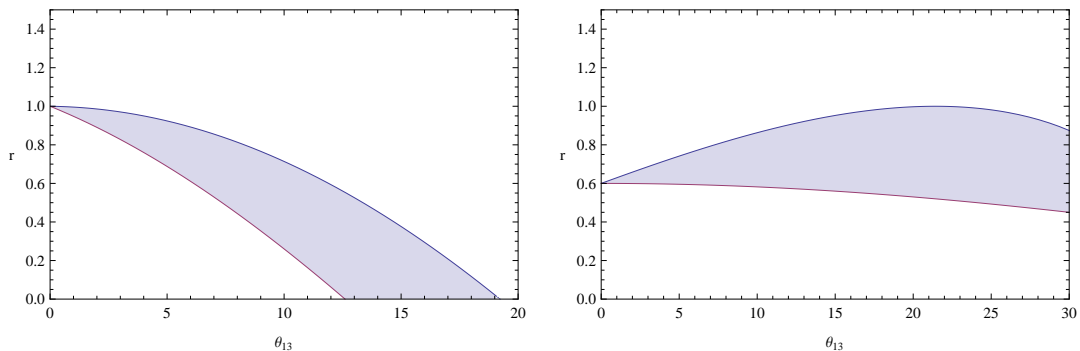


FIG. 6. The inconsistency between r and θ_{13} (degrees) for patterns B_1 (left) and B_3 (right).

[arXiv:1706.02017 [hep-ph]].

[8] C. Jarlskog, *Phys. Rev. Lett.* **55**, 1039 (1985).

[9] R. R. Gautam and S. Kumar, *Phys. Rev. D* **94**, no. 3, 036004 (2016), [arXiv:1607.08328 [hep-ph]].

[10] I. Esteban, M. C. Gonzalez-Garcia, M. Maltoni, I. Martinez-Soler and T. Schwetz, *JHEP* **1701**, 087 (2017), [arXiv:1611.01514 [hep-ph]].

[11] K. Iwamoto, Recent Results from T2K and Future Prospects. Talk given at the 38th International Conference on High Energy Physics, Chicago, USA, August 3–10, 2016; P. Vahle, New results from NOvA. Talk given at the XXVII International Conference on Neutrino Physics and Astrophysics, London, UK, July 49, 2016.